

Supporting Information

Nanoscale Engineering of Nitrogen-doped Carbon Nanofiber Aerogels for Enhanced Lithium Ion Storage

Guichao Ye, Xiaoyi Zhu, Shuai Chen, Daohao Li, Yafang Yin, Yun Lu,*

Sridhar Komarneni, Dongjiang Yang*

Email: y.lu@criwi.org.cn; d.yang@qdu.edu.cn

Experimental Section

Materials Synthesis: The bleached bamboo pulps were purchased from Tianjin wood elf Biotechnology Co., Ltd. Potassium hydroxide and hydrochloric acid were purchased from Aladdin Co. Other chemicals were supplied by Shanghai Boyle chemical Co. Ltd. All the reagents were used without any further purification after purchase. After mechanical milling treatment, the processed cellulose was dispersed in distilled water with 1000 mL of the water slurry containing 0.01 wt% samples. Then, sonication was performed with a common ultrasonic generator (JY99-IIID, Ningbo Scientz Biotechnology Co., Ltd., China). The subsequent ultrasonic experiments were performed under a 50% duty cycle in order to reduce temperature variation, and conducted for an optimum time length with an output power of 1,500 W to disperse and isolate the fibers. The unfibrillated fraction (<10%) was removed by centrifugation, and the supernatant was used as the nanofibers of cellulose (NFC) or nanofibrillated cellulose dispersions. After that, the suspensions were treated with tert-butyl alcohol for 24 h followed by freezing in liquid nitrogen for 20 min and freeze dried with a freeze drier at -80 °C for 72 h in a vacuum (~10 Pa). Then the formed NFC aerogels were placed in a tubular furnace and heated from room temperature to 250 °C at a heating rate of 2 °C/min. The aerogels were treated for 2 h in air 250 °C. The as-stabilized nanofibers were subsequently heated to 800 °C at the heating rate of 5 °C/min in nitrogen or ammonia

atmosphere to obtain 3D carbon nanofibers (CNF) or N-doped carbon nanofibers (N-CNF). In addition, the CNF or N-CNF were activated with KOH in nitrogen gas with a flow rate of 80 ml/min to form the KOH activated CNFs (ACNF) or KOH activated N-CNF (denoted as N-ACNF) before measuring their electrochemical properties.

Sample Characterization: The phase formation of the samples was characterized by X-ray diffraction using an X-ray diffractometer (Bruker D8 Adv, Germany). Morphology of the samples was determined by a transmission electron microscope (FEI Tecnai G20, USA), a high-resolution transmission electron microscope (FEI Tecnai G20, USA) and a field-emission scanning electron microscope (Tecnai G2 F20, USA). An X-ray photoelectron spectrometer (Thermo ESCALAB 250XI, USA) was used to collect XPS data and a TG analyzer (TA Q600, USA) was used to determine weight loss. Specific surface area was calculated by the Brunauer-Emmett-Teller method (AutoChem II 2920, USA) from the data in a relative pressure (P/P_0) range between 0.05 and 0.20 and pore size distribution plots were derived from the adsorption branch of the isotherms based on the BJH model.

Electrochemical Measurements: The samples were mixed with acetylene black and poly (vinylidene fluoride) (PVDF) at a weight ratio of 8:1:1 in N-methyl-2-pyrrolidone (NMP) solvent to form the slurry. Then, the resultant slurry was uniformly pasted on Cu foil substrate. The as-prepared electrode sheet was dried in a vacuum oven at 120 °C for 10 h and then pressed. The electrolyte consisted of a solution of 1 M LiPF₆ in ethylene carbonate (EC)/dimethyl carbonate (DMC)/diethyl carbonate (DEC) (1:1:1, in wt%). CR2016-type coin cells were assembled in a glove box for electrochemical characterization. Lithium metal foil was used as both the counter and reference electrodes. The charge-discharge measurements were conducted using a cell testing instrument (LAND CT2001A) over the potential range from 0.01 to 3.00 V. Cyclic voltammetry (CV) (0.01 V to 3.0 V, 0.1 mV s⁻¹) was performed using a CHI 760 E electrochemical workstation (CH Instruments, Inc.).

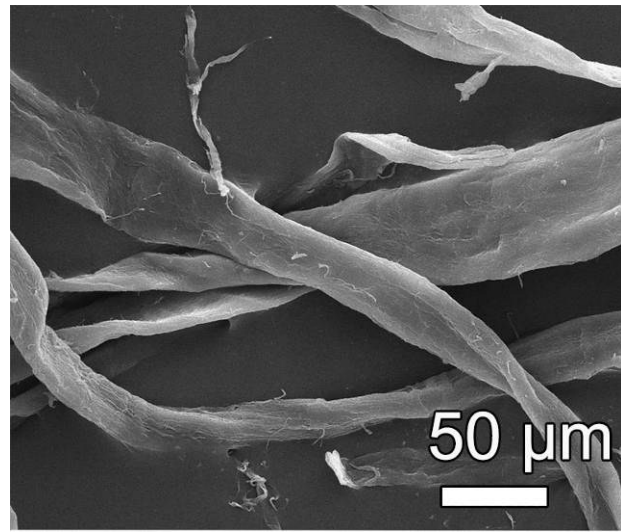


Fig. S1 FESEM image of bamboo pulp

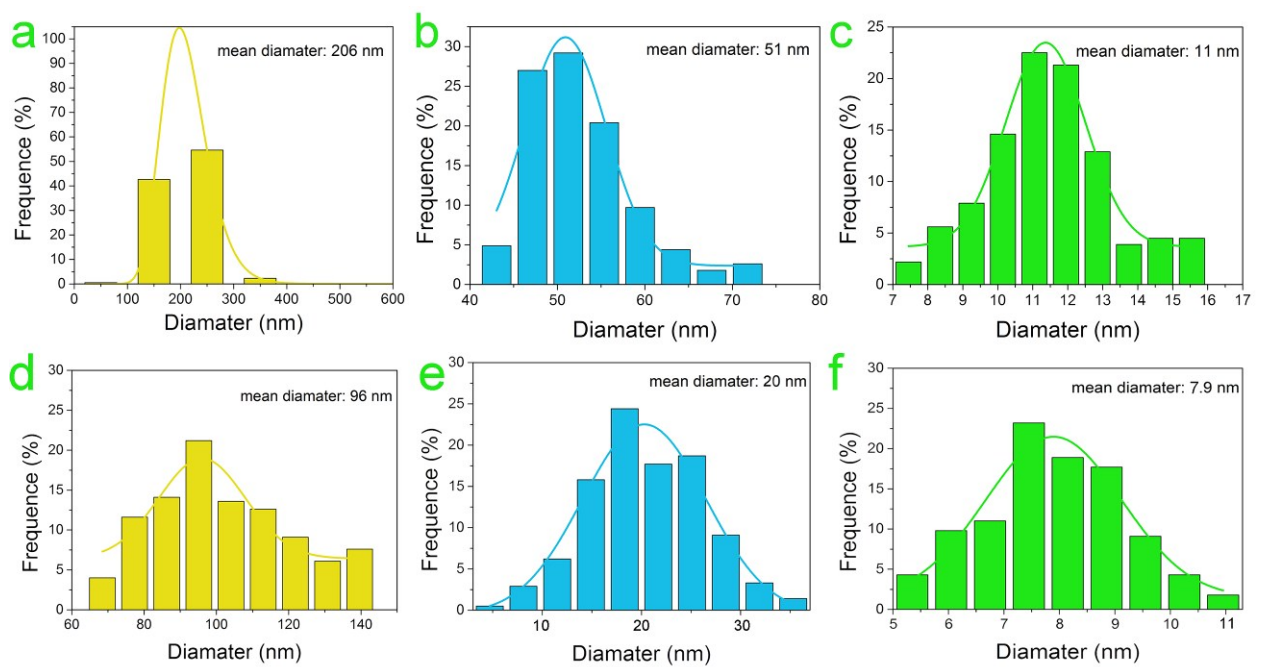


Fig. S2 The measured diameter distribution ($n=200$) histograms of (a) NFC-200, (b) NFC-50, (c) NFC-10, (d) CNF-200, (e) CNF-50, (f) CNF-10.

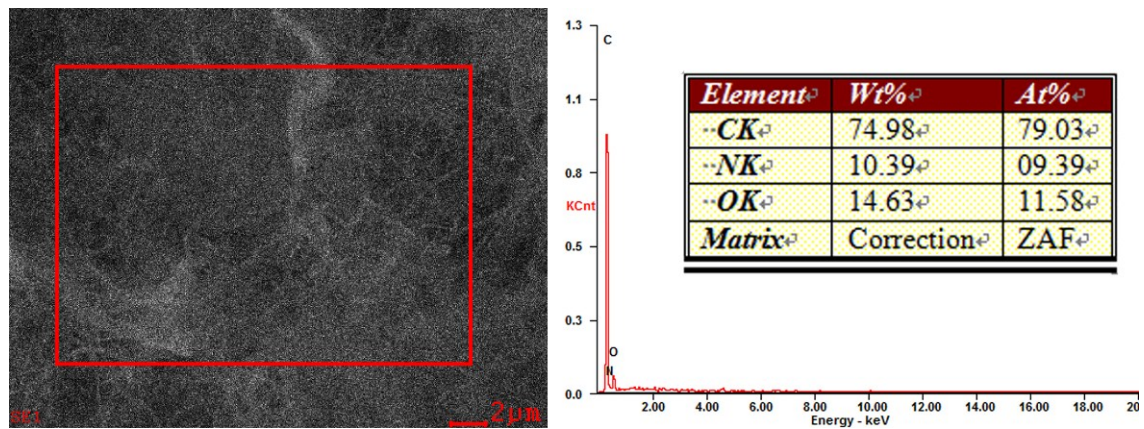


Fig. S3 Elemental distribution on the surface of N-ACNF-50

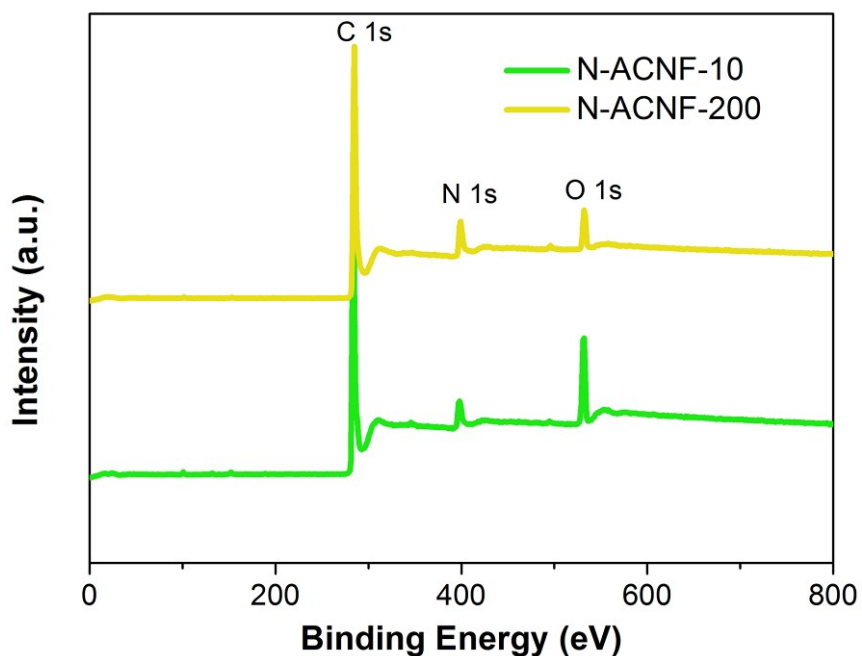


Fig. S4 XPS spectra of N-ACNF-10, 200 aerogel: full survey scan spectrum.

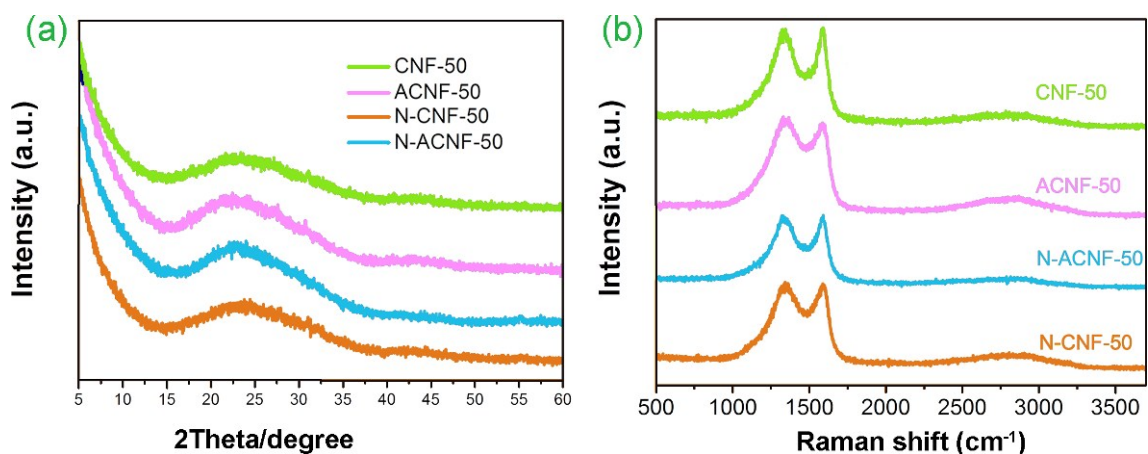


Fig. S5 a) XRD patterns of CNF-50, ACNF-50, N-CNF-50 and N-ACNF-50 aerogels. b) Raman spectra of CNF-50, ACNF-50, N-CNF-50 and N-ACNF-50 aerogels.

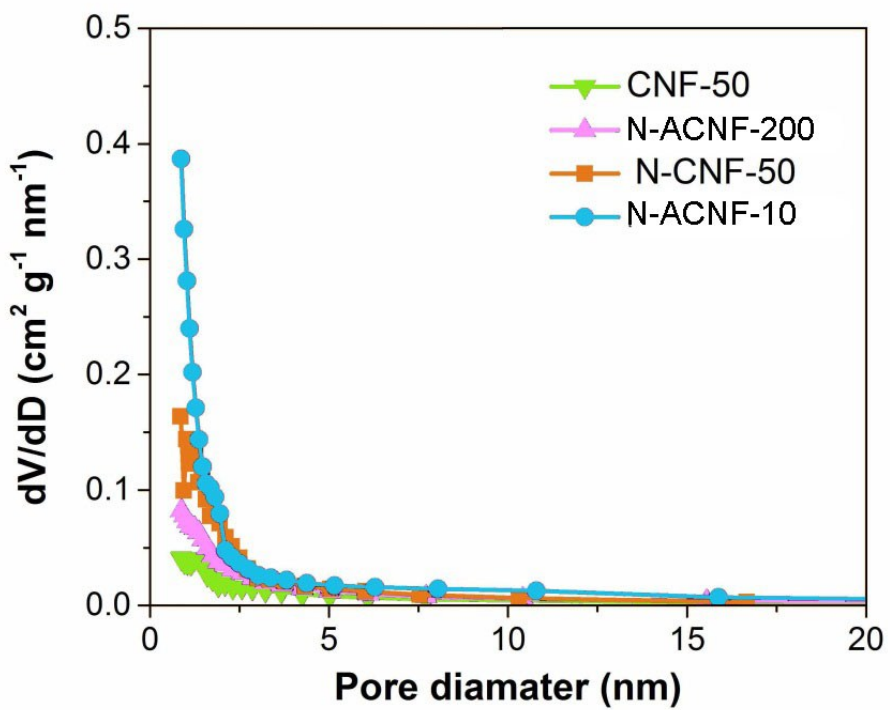


Fig. S6 pore size distributions of N-ACNF-200, N-ACNF-50 and N-ACNF-10 aerogels.

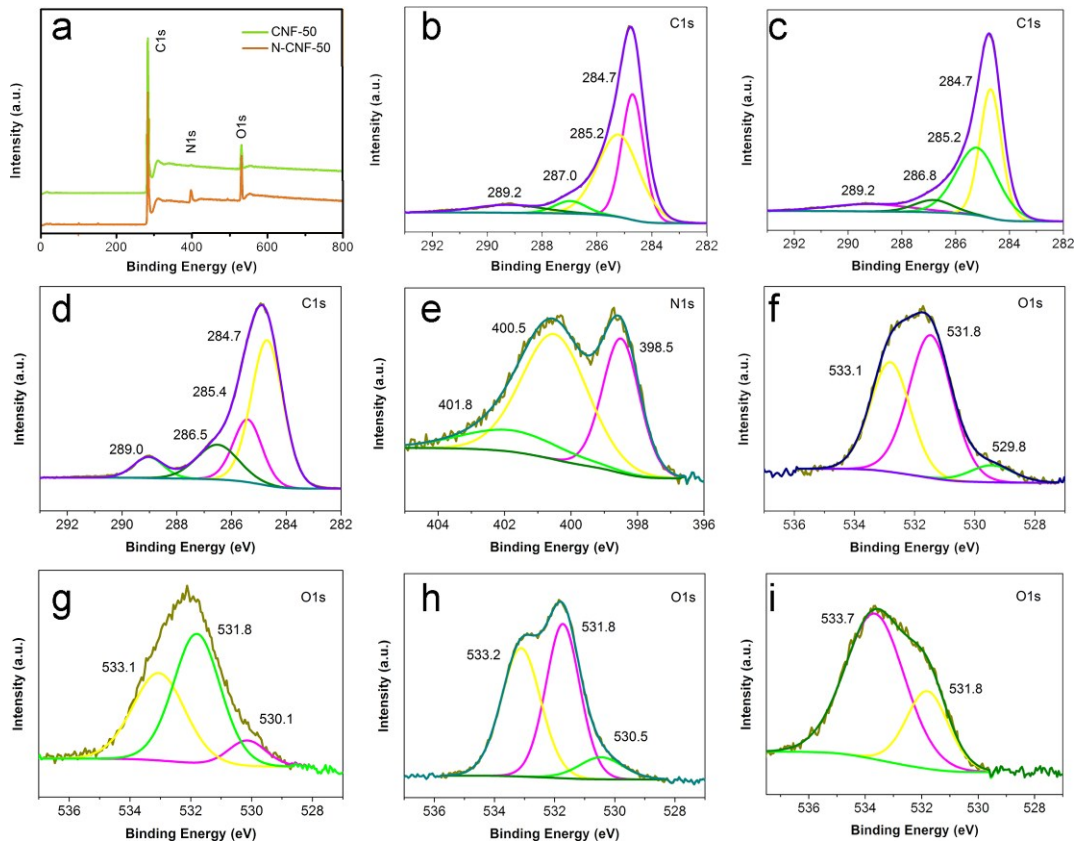


Fig. S7 (a) Survey XPS spectra of CNF and N-CNF aerogels. High-resolution XPS spectra of (b) C_{1s} and (f) O_{1s} in CNF aerogel; (c) C_{1s} and (g) O_{1s} in ACNF aerogel; (d) C_{1s}, (e) N_{1s} and (h) O_{1s} in N-CNF aerogel; (i) O_{1s} in N-ACNF aerogel.

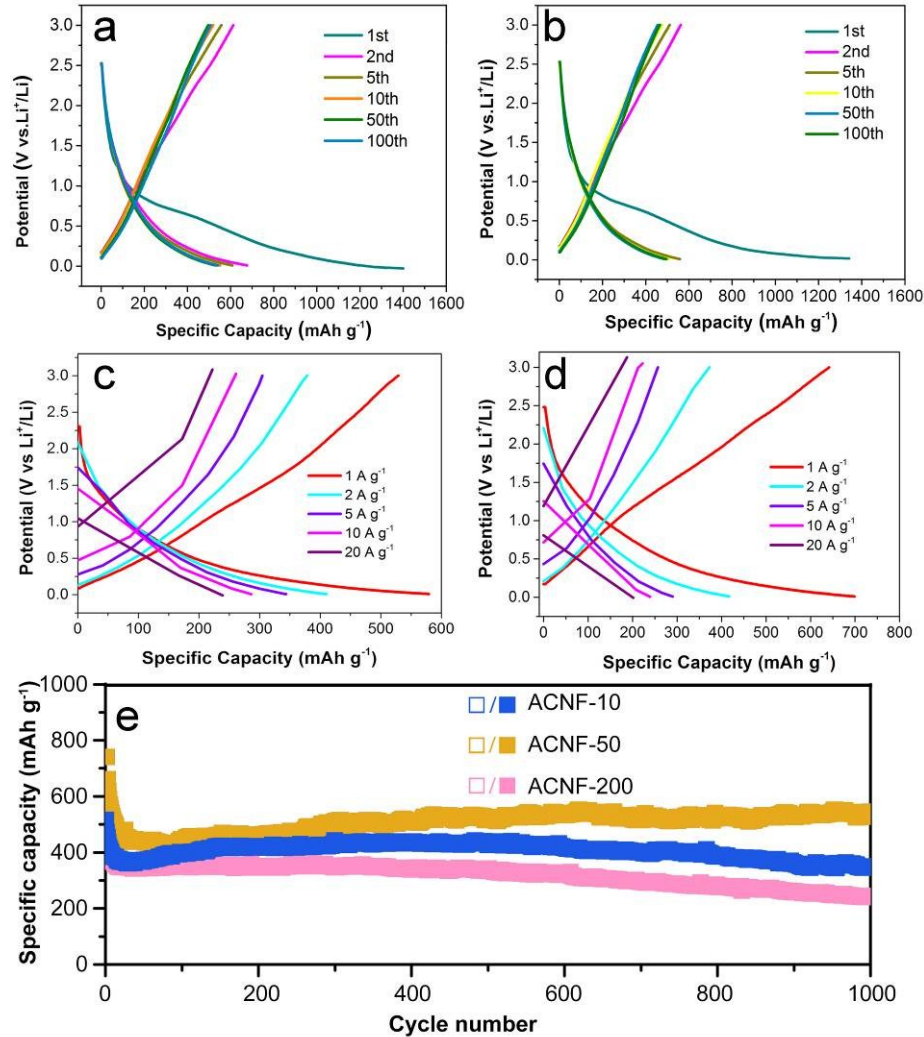


Fig. S8 The charge and discharge curves of (a) N-ACNFs-10 and (b) N-ACNF-200 aerogels cycled at the 1st, 2nd, 5th, 10th, 50th, 100th between 0.01 and 3.0 V (vs. Li⁺/Li) at a current density of 1 A g⁻¹. (c) Discharge/charge voltage curves of ACNF-50 at different rates from 1 A g⁻¹ to 20 A g⁻¹. (d) Discharge/charge voltage curves of CNF-50 at different rates from 1 A g⁻¹ to 20 A g⁻¹. (e) Long-term cycling performance of ACNF-10, ACNF-50, ACNF-200 aerogels at a current density of 1 A g⁻¹.

Table S1. The atomic percentages of C, N and O for N-ACNF-50, N-CNF-50, CNF-50 and ACNF-50 aerogels

Item	N-ACNF-50	N-CNF-50	CNF-50	ACNF-50
C-contents (at%)	85.6	80.0	93.6	93.4
N-contents (at%)	7.3	7.1	0	0
O-contents (at%)	7.1	11.9	6.4	6.6

Table S2. Comparison of LIBs performance of N-ACNF-50 with the state-of-the-art carbonaceous materials reported recently.

Reference Number	Material	Cyclability			Rate performance (Capacity/mAh g ⁻¹)		
		Capacity (mAh g ⁻¹)	Cycle number	Current density (A g ⁻¹)	1 A g ⁻¹	2 A g ⁻¹	5 A g ⁻¹
This work	N-ACNF-50	651	1000	1	631	487	418
Ref. S1	Hollow Carbon Nanospheres	630	50	0.0372	337	229	<133
Ref. S2	N-doped Hollow Carbon Nanoflowers	528	1000	0.744	564	384	<298
Ref. S3	Porous Carbon/Graphene	620	100	0.1	/	/	250
Ref. S4	Expanded Graphite	400	300	0.1	270	/	/
Ref. S5	Cellulose-derived Porous Carbon	447	800	1	625	500	/
Ref. S6	Porous Carbon Nanofiber Webs	549	100	1	505	436	/
Ref. S7	Micro-sized Porous Carbon Spheres	507	100	0.1	305	280	345
Ref. S8	Carbon Derived from Banana Peel	717	300	0.1	518	385	243
Ref. S9	Reduced Graphene Foam	470	600	0.186	330	/	/
Ref. S10	Hard Carbon Nanofibers	255	200	0.2	210	155	/
Ref. S11	N-rich Porous Carbon Spheres	540	100	0.5	410	293	/

Table S3 Summary of the fitting results for N_{1s} spectrum of the as-prepared N-ACNF-50 aerogel.

Pyridinic N		Pyrrolic N		Quaternary N	
Content (%)	Position (eV)	Content (%)	Position (eV)	Content (%)	Position (eV)
32.37	398.5	53.57	400.5	14.06	401.8

Reference

S1. F.-D. Han, Y.-J. Bai, R. Liu, B. Yao, Y.-X. Qi, N. Lun, J.-X. Zhang, *Adv. Energy Mater.* 2011, **1**, 798-801.

S2. C. Qian, P. Guo, X. Zhang, R. Zhao, Q. Wu, L. Huan, S. Xiao, M. Chen, *RSC Advances*. 2016, **6**, 93519-93524.

S3. R. Guo, L. Zhao, W. Yue, *Electrochimica Acta*. 2015, **152**, 338-344.

S4. T. Zhao, S. She, X. Ji, X. Guo, W. Jin, R. Zhu, A. Dang, H. Li, T.-H. Li, B.-Q. Wei, *Sci Reports*. 2016, **6**.

S5. C. Zhu, T. Akiyama, *Green Chem.* 2016, **18**, 2106-2114.

S6. W. Wang, Y. Sun, B. Liu, S. Wang, M. Cao, *Carbon*. 2015, **91**, 56-65.

S7. M. Chen, C. Yu, S. Liu, X. Fan, C. Zhao, X. Zhang, J. Qiu, *Nanoscale*. 2015, **7**, 1791-1795.

S8. E. M. Lotfabad, J. Ding, K. Cui, A. Kohandehghan, W. P. Kalisvaart, M. Hazelton, D. Mitlin, *ACS Nano*. 2014, **8**, 7115-7129.

S9. J. Yao, B. Liu, S. Ozden, J. Wu, S. Yang, M. T. F. Rodrigues, K. K. Pei, D.-P Xiao, Y.-H. Zhang, R. V. Pulickel, M. Ajayan, *Electrochimica Acta*. 2015, **176**, 103-111.

S10. Z. Shi, C. Chong, J. Wang, C. Wang, X. Yu, *Mater Letter*. 2015, **159**, 341-344.

S11. D. Li, L.-X. Ding, H. Chen, S. Wang, Z. Li, M. Zhu and H. Wang, *J. Mater. Chem. A*. 2014, **2**, 16617-16622.